

Correlations of electromagnetic fields in chaotic cavities

B. Eckhardt, U. Dörr, U. Kuhl and H.-J. Stöckmann

Fachbereich Physik, Philipps Universität Marburg, D-35032 Marburg, Germany

We consider the fluctuations of electromagnetic fields in chaotic microwave cavities. We calculate the transversal and longitudinal correlation function based on a random wave assumption and compare the predictions with measurements on two- and three-dimensional microwave cavities.

Classical ergodicity suggests that wave functions in chaotic systems may be described by superpositions of waves with wave vectors of constant length but random directions [1,2]. Their fluctuations are distinctly different from the more familiar optical speckle patterns where also the wave numbers fluctuate [3]. The distributions of amplitudes turns out to be Gaussian and the spatial auto-correlation function is given by Bessel functions of order $\frac{d}{2} - 1$, where d is the billiard dimension. Overwhelming evidence for this has been accumulated especially in numerical studies of billiards [4–6], experiments on microwave billiards [7,8] and surfaces of constant negative curvature [9]. Higher order moments and correlations [10,11] as well as contributions from prominent classical structures ('scars') have also been studied [12], so that by now one has a fairly good understanding of the fluctuation properties of scalar wave functions in chaotic systems.

Recent experiments on the elastodynamics of vibrating blocks [13] and 3-d microwave resonators [14,15] deal with situations where the wave fields have more than one component which are typically mixed by the boundary conditions [16–19]. New effects such as ray splitting [18] or chaotic features in systems with integrable ray dynamics [19] are found.

We are here interested in the consequences of these additional degrees of freedom for the fluctuations of the wave functions. In particular, we will show that the fact that in the absence of space charges electromagnetic fields are divergence free implies differences between the longitudinal and transversal correlation functions and deviations from the behaviour expected for scalar fields [2]. We present results for the field components, the intensities and the frequency shift and compare with experiments on microwave billiards.

Our starting point is the electromagnetic analog of the semiclassical ansatz that the scalar field is a superposition of plane waves with constant amplitudes and fixed wave length but randomly oriented wave vector [2]. For the electromagnetic case we have in addition to allow for different orientations of the polarization. We thus assume that the field at a point \mathbf{x} in position space is due to a superposition of many plane waves with uniformly distributed orientations of polarization and wave vector, e.g.,

$$\mathbf{E}(\mathbf{x}) \approx \sum_{\nu} \mathbf{E}_{\nu} e^{i\mathbf{k}_{\nu} \cdot \mathbf{x}}, \quad (1)$$

and similarly for the \mathbf{B} -field. The complex amplitudes

\mathbf{E}_{ν} and \mathbf{B}_{ν} of all waves are transversal, $\mathbf{E}_{\nu} \cdot \mathbf{k}_{\nu} = 0$ and $\mathbf{B}_{\nu} \cdot \mathbf{k}_{\nu} = 0$, and satisfy $\mathbf{E}_{\nu} \cdot \mathbf{B}_{\nu} = 0$ so that \mathbf{k}_{ν} , \mathbf{E}_{ν} and \mathbf{B}_{ν} form an orthogonal dreibein. The absolute values $|\mathbf{E}_{\nu}|$ and $|\mathbf{B}_{\nu}|$ are all the same, that is to say, we assume that there are no losses during reflections at the walls. From this assumption there follows immediately that all three components are Gaussian distributed with the same distribution [14]

The spatially averaged correlation functions then are for the electric field

$$C_{E,ij}(\mathbf{r}) = \langle \mathbf{E}_i(\mathbf{x} + \mathbf{r}/2) \mathbf{E}_j(\mathbf{x} - \mathbf{r}/2) \rangle / \langle \mathbf{E}_i^2 \rangle, \quad (2)$$

and similar for the magnetic field and the cross correlation between \mathbf{E} and \mathbf{B} . The normalization is by the mean square amplitude of a single component of the fields, $\langle \mathbf{E}_i^2 \rangle$, so that $C_{E,ii}(0) = 1$. In a tensor notation, this can be combined to a tensor of correlation functions,

$$C_E(\mathbf{r}) = \langle \mathbf{E}(\mathbf{x} + \mathbf{r}/2) \otimes \mathbf{E}(\mathbf{x} - \mathbf{r}/2) \rangle / \langle \mathbf{E}_i^2 \rangle. \quad (3)$$

Substituting (1) and performing the spatial average then results in (the normalization will be restored in the end)

$$C_E(\mathbf{r}) \propto \sum_{\nu} \mathbf{E}_{\nu} \otimes \mathbf{E}_{\nu}^* e^{i\mathbf{k}_{\nu} \cdot \mathbf{r}}. \quad (4)$$

To proceed further, let \mathbf{r} point in the z -direction and introduce spherical coordinates for the wave vector,

$$\mathbf{k}_{\nu} = k \begin{pmatrix} \cos \phi_{\nu} \sin \theta_{\nu} \\ \sin \phi_{\nu} \sin \theta_{\nu} \\ \cos \theta_{\nu} \end{pmatrix}. \quad (5)$$

The electromagnetic field contributions lie in a plane perpendicular to this wave vector, spanned by the two vectors

$$\mathbf{e}_1^{(\nu)} = \begin{pmatrix} -\sin \phi_{\nu} \\ \cos \phi_{\nu} \\ 0 \end{pmatrix}, \quad \mathbf{e}_2^{(\nu)} = \begin{pmatrix} -\cos \phi_{\nu} \cos \theta_{\nu} \\ -\sin \phi_{\nu} \cos \theta_{\nu} \\ \sin \theta_{\nu} \end{pmatrix}. \quad (6)$$

If ψ_{ν} denotes the angle of polarization, the field components are

$$\mathbf{E}_{\nu} = \cos \psi_{\nu} \mathbf{e}_1^{(\nu)} + \sin \psi_{\nu} \mathbf{e}_2^{(\nu)} \quad (7)$$

$$\mathbf{B}_{\nu} = -\sin \psi_{\nu} \mathbf{e}_1^{(\nu)} + \cos \psi_{\nu} \mathbf{e}_2^{(\nu)}. \quad (8)$$

In the limit of a large number of contributing components, the sum over the different contributions can be

replaced by a continuous average over all directions (angles θ and ϕ) for the wave vector and all polarizations (angle ψ),

$$\frac{1}{N} \sum_{\nu} \dots \rightarrow \frac{1}{2\pi} \int_0^{2\pi} d\psi \frac{1}{2\pi} \int_0^{2\pi} d\phi \frac{1}{2} \int_0^{\pi} \sin\theta d\theta \dots \quad (9)$$

After averaging over the polarizations and the azimuthal angle, the correlation functions become

$$C_E(\mathbf{r}) = \frac{3}{4} \begin{pmatrix} 1 & 0 & 0 \\ 0 & 1 & 0 \\ 0 & 0 & 0 \end{pmatrix} \langle e^{i\mathbf{k}\mathbf{r} \cos\theta} \rangle_{\theta} + \left\langle \begin{pmatrix} \frac{3}{4} \cos^2\theta & 0 & 0 \\ 0 & \frac{3}{4} \cos^2\theta & 0 \\ 0 & 0 & \frac{3}{2} \sin^2\theta \end{pmatrix} e^{i\mathbf{k}\mathbf{r} \cos\theta} \right\rangle_{\theta}. \quad (10)$$

The final average over θ can be expressed in terms of spherical Bessel functions, but it is more convenient to use the trigonometric representation directly,

$$C_E(\mathbf{r}) = \begin{pmatrix} f_{\perp}(kr) & 0 & 0 \\ 0 & f_{\perp}(kr) & 0 \\ 0 & 0 & f_{\parallel}(kr) \end{pmatrix} \quad (11)$$

with the transversal correlation function

$$f_{\perp}(\xi) = \frac{3}{2} \left(\frac{\sin \xi}{\xi} - \frac{\sin \xi - \xi \cos \xi}{\xi^3} \right) \quad (12)$$

and the longitudinal correlation function

$$f_{\parallel}(\xi) = 3 \frac{\sin \xi - \xi \cos \xi}{\xi^3}. \quad (13)$$

The asymptotic behaviour of these functions is that for small r they approach the same value, $C_{E,ii} \rightarrow 1$, by normalization. For large r they oscillate on a scale set by the wavenumber and decay like $1/r$ for the transversal and like $1/r^2$ for the longitudinal correlations. For the trace of the correlation function,

$$\text{tr } C_E = \langle \mathbf{E}(\mathbf{x} + \mathbf{r}/2) \cdot \mathbf{E}(\mathbf{x} - \mathbf{r}/2) \rangle / \langle \mathbf{E}_i^2 \rangle \quad (14)$$

$$= 3 \frac{\sin kr}{kr} \quad (15)$$

the correlation between polarizations and wave vector is eliminated and one recovers Berry's result for random waves in three dimensions [2], except for a factor due to the normalization (see Fig. 1).

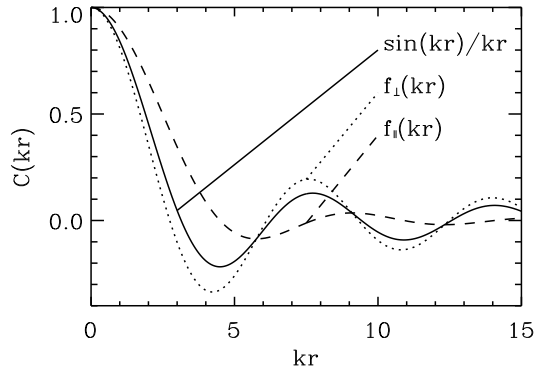


FIG. 1. Correlation functions for longitudinal and transversal fluctuations (dashed and dotted line, respectively) for the electromagnetic fields. The full line shows the correlation function for a 3-d scalar wave function for comparison.

The correlations for the magnetic field \mathbf{B} have the same functional dependence,

$$C_B(\mathbf{r}) = \begin{pmatrix} f_{\perp}(kr) & 0 & 0 \\ 0 & f_{\perp}(kr) & 0 \\ 0 & 0 & f_{\parallel}(kr) \end{pmatrix}. \quad (16)$$

There are no correlations between \mathbf{E} and \mathbf{B} .

For the experiments also the correlations of intensities,

$$C_{EE}(\mathbf{r}) = \langle |\mathbf{E}(\mathbf{x} + \mathbf{r}/2)|^2 |\mathbf{E}(\mathbf{x} - \mathbf{r}/2)|^2 \rangle / \langle |\mathbf{E}|^4 \rangle \quad (17)$$

and similarly for the magnetic field are relevant. For ease of comparison with numerical data, we normalize this function by the second moment of the intensity so that $C \rightarrow 1$ as $\mathbf{r} \rightarrow 0$. For large \mathbf{r} the correlations between intensities decay and the correlation function approaches $\langle |\mathbf{E}|^2 \rangle^2 / \langle |\mathbf{E}|^4 \rangle$. For Gaussian random field components, this ratio is $3/5$. Therefore, the correlation function with the above normalization becomes

$$C_{EE}(\mathbf{r}) = \frac{4}{15} [f_{\perp}(kr)]^2 + \frac{2}{15} [f_{\parallel}(kr)]^2 + \frac{9}{15} \quad (18)$$

and similar for the magnetic field. For the intensity correlation function of a 3-d scalar field the correlation function becomes

$$C_{ss}(\mathbf{r}) = \frac{2}{3} \left(\frac{\sin kr}{kr} \right)^2 + \frac{1}{3}, \quad (19)$$

where the asymptotic value of $1/3$ reflects the ratio of the square of the second moment to the fourth moment as expected for a Gaussian distribution [10,11].

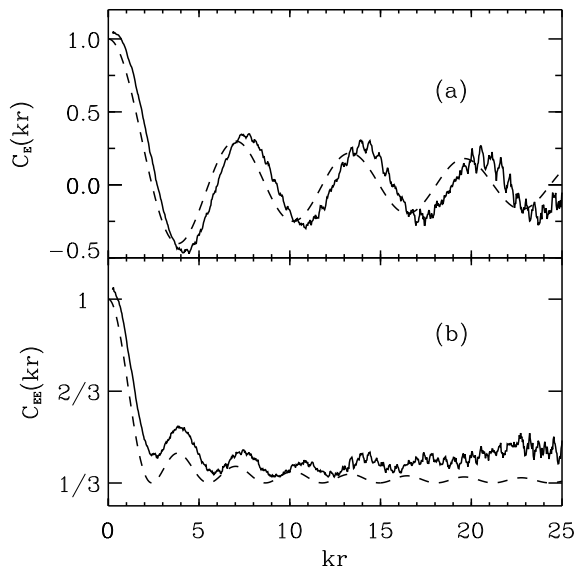


FIG. 2. Comparison between experimental results for spatial autocorrelation functions in a quarter stadium microwave billiards and theory. The experimental curves were obtained by superimposing the results for the 20 lowest lying eigenresonances. (a) Spatial autocorrelation function of the electric field amplitudes (full line) and theoretical predictions from Eq. (20). (b) Spatial autocorrelation function for the squares of the electric field amplitudes using the same data set as in (a). The dashed line corresponds to the prediction from Eq. (21).

To test these predictions we measured the field distributions in two- and three-dimensional microwave billiards. We start with the discussion of the results in a resonator of the shape of a quarter stadium billiard. We measured the microwave transition amplitudes between two antennas, one kept fixed, the other moved around to probe the spatial distribution of the wave functions. At an eigenfrequency such measurements yield directly the electric field strength $\mathbf{E}(x)$ as a function of the position. Details of the experiment are described elsewhere [20]. For microwave frequencies below $\nu_{max} = c/2d$, where d is the height of the resonator, only TM modes are excited and the electric field has a single component E_z . For this component, Berry's arguments give a spatial autocorrelation function

$$C_E(\mathbf{r}) = \langle E_z(\mathbf{x} + \mathbf{r}/2) \cdot E_z(\mathbf{x} - \mathbf{r}/2) \rangle \sim J_0(kr) \quad (20)$$

Fig. 2(a) shows the experimental autocorrelation function, normalized to $C_E(0) = 1$. It was obtained by superimposing the results from the 20 lowest eigenfrequencies of the quarter stadium. Apart from a discrepancy of about 10 percent in the wavelength of the oscillations the experiment reproduces the prediction by Eq. (20) perfectly.

The autocorrelation function of the field intensities becomes in the 2-d case

$$C_{EE}(\mathbf{r}) = \langle |E_z(\mathbf{x} + \mathbf{r}/2)|^2 |E_z(\mathbf{x} - \mathbf{r}/2)|^2 \rangle$$

$$\sim \frac{2}{3} [J_0(kr)]^2 + \frac{1}{3}. \quad (21)$$

This correlation function, which has also been studied by Sridhar et al. [7], is shown in Fig. 2(b) for the same data set that entered Fig. 2(a). As in Fig. 2(a) we note a small difference in the wavelength of the oscillations. This has not been observed in the experiments of Sridhar et al. [7] and in the stadium wave functions in Ref. [5], but it has appeared for wave functions of an octogon billiard on a surface with constant negative curvature [9], where it has been attributed to anisotropies in the wave functions. In the present case the discrepancy may be caused by higher order corrections to the semiclassical predictions since the wave functions are not very far into the semiclassical regime: Typical wave lengths for the wave functions that entered the analysis of Fig. 2 are about 0.2–0.5 stadium widths. Assuming corrections to be of order $1/k^2$ with a prefactor of order 1, as suggested by the analysis of [21], the deviations can be estimated to be about 10%, as observed.

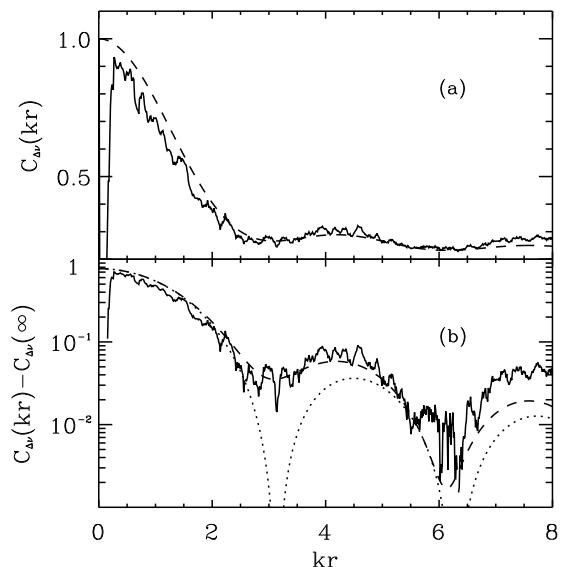


FIG. 3. Spatial autocorrelation function $C_{\Delta\nu}(kr)$ for the frequency shifts obtained by the perturbing bead method in a three-dimensional Sinai billiard. The dashed line corresponds to the theoretical prediction from Eq. (23), taking into account the vector properties of the electromagnetic fields. (a) Correlation function on a linear scale. (b) The correlation function $C_{\Delta\nu}(kr) - C_{\Delta\nu}(\infty)$ on a logarithmic plot. The dotted line corresponds to Eq. (19) and would have been expected for three-dimensional scalar fields.

Turning to the three-dimensional microwave cavities note that Maxwell's equations can no longer be reduced to a scalar wave equation, so that effects due to the vector properties of the electromagnetic field can become essential. The field distributions in a cavity of the shape of a three-dimensional Sinai billiard were mapped by means

of the perturbing bead method [14]. The technique uses the fact that a spherical metallic bead in the resonator shifts the eigenfrequency of a resonance by an amount $\Delta\nu$ proportional to $-2\mathbf{E}^2 + \mathbf{B}^2$, where \mathbf{E} and \mathbf{B} are the fields at the position of the bead. Since the electric and the magnetic field components are uncorrelated, the spatial autocorrelation function for the frequency shift,

$$C_{\Delta\nu}(r) = \langle \Delta\nu(\mathbf{x} + \mathbf{r}/2) \cdot \Delta\nu(\mathbf{x} - \mathbf{r}/2) \rangle \quad (22)$$

is given by the intensity autocorrelation function defined in Eq. (18), up to an off-set resulting from the fact that $C_{\Delta\nu}(r)$ does not vanish in the limit $r \rightarrow \infty$. This off-set is easily calculated. Using again that for Gaussian distributions the fourth moment amounts to three times the square of the second moment, we find $C_{\Delta\nu}(0)/C_{\Delta\nu}(\infty) = 13/3$. After normalization we thus have

$$C_{\Delta\nu}(r) = \frac{20}{39} [f_{\perp}(kr)]^2 + \frac{10}{39} [f_{\parallel}(kr)]^2 + \frac{3}{13} \quad (23)$$

The experimental results in Fig. 3(a) are in good agreement with the theoretical prediction from Eq. (23) for kr -values below 6. The hole in the histogram for $kr < 0.2$ reflects the minimum grid size used in the bead measurement. In Fig. 3(b) the data for $C_{\Delta\nu}(r) - C_{\Delta\nu}(\infty)$ are replotted on a logarithmic scale to emphasize the minima. Also shown is the scalar correlator (19). Note that the scalar function has zeroes but the spectral correlator does not. The absence of zeroes or, in the case of finite resolution, deep minima, in the experimental data is thus clear evidence for the influence of the polarizations.

In summary, we have shown that longitudinal and transversal correlation functions of electromagnetic waves in chaotic cavities differ because the waves are transversal. The experiments verified the effect for the intensities, and more direct studies of the fields themselves are desirable. We expect that also in other situations with non-scalar waves fields, as for instance in acoustics in anisotropic media or hydrodynamic waves, the correlations will be characterized by tensors which depend on the character of the modes and the directions.

This work was partially supported by the Deutsche Forschungsgemeinschaft through Sonderforschungsbereich 185 'Nichtlineare Dynamik'.

-
- [1] A. Voros, Ann. Inst. Henri Poincaré, Sect A, **26**, 343 (1977)
 - [2] M. Berry, J. Phys. A **10**, 2083 (1977)
 - [3] P. O'Connor, J. Gehlen, and E. Heller, Phys. Rev. Lett. **58**, 1296 (1987)
 - [4] S. McDonald and A. Kaufmann, Phys. Rev. Lett. **42**, 1189 (1979)
 - [5] S. McDonald and A. Kaufmann, Phys. Rev. A **37**, 3067 (1988)
 - [6] M. Shapiro and G. Goelman, Phys. Rev. Lett. **53**, 1714 (1984)
 - [7] A. Kudrolli, V. Kidambi, and S. Sridhar, Phys. Rev. Lett. **75**, 822 (1995)
 - [8] V. Prigodin *et al.*, Phys. Rev. Lett. **75**, 2392 (1995)
 - [9] R. Aurich and F. Steiner, Physica D **64**, 185 (1993)
 - [10] M. Srednicki, Phys. Rev. E **54**, 954 (1996)
 - [11] M. Srednicki and F. Stiernelof, J. Phys. A **29**, 5817 (1996)
 - [12] E.J. Heller, Phys. Rev. Lett. **53**, 1515 (1984)
 - [13] C. Ellegaard *et al.*, Phys. Rev. Lett. **77**, 4918 (1996)
 - [14] U. Dörr, H.-J. Stöckmann, M. Barth, and U. Kuhl, Phys. Rev. Lett. **80**, 1030 (1998)
 - [15] H. Alt *et al.*, Phys. Rev. Lett. **79**, 1026 (1997)
 - [16] R. Balian and C. Duplantier, Ann. Phys. **64**, 271 (1971)
 - [17] O. Frank and B. Eckhardt, Phys. Rev. E **53**, 4166 (1996)
 - [18] L. Couchman, T.M. Antonsen and E. Ott, Phys. Rev. A **46**, 6193 (1992)
 - [19] R. L. Weaver, J. Acoust. Soc. Am. **85**, 1005 (1989)
 - [20] J. Stein, H.-J. Stöckmann, and U. Stoffregen, Phys. Rev. Lett. **75**, 53 (1995)
 - [21] P. Gaspard and D. Alonso, Phys. Rev. E **47**, 3468 (1993)